Available online at www.sciencedirect.com
ScienceDirect
Journal of Sound and Vibration 305 (2007) 945–955
JOURNAL OF SOUND AND VIBRATION
www.elsevier.com/locate/jsvi

Short Communication

The connection between effective independence and modal kinetic energy methods for sensor placement

D.S. Li[a,b,*], H.N. Li[a], C.P. Fritzen[b]

[a]*Dalian University of Technology, State Key Laboratory of Coastal and Offshore Engineering, Linggong RD.2, Dalian 116023, China*
[b]*University of Siegen, Institute of Mechanics and Automatic Control-Mechatronics, Paul-Bonatz Str. 9-11, D-57076 Siegen, Germany*

Received 26 January 2007; received in revised form 12 April 2007; accepted 3 May 2007
Available online 21 June 2007

Abstract

The comparison and inherent relationship between two influencing sensor placement methods, i.e. modal kinetic energy (MKE) and effective independence (EI), are addressed in this paper. The problem is of primary concern for dynamic testing, damage identification and structural health monitoring. By analyzing the sensor placement problem with EI method from the perspective of a new reduced system, the connection of MKE with EI method is revealed. The latter is an iterated version of the former, and the reduced mode shapes are ortho-normalized repeatedly during iterations of the latter. Two alternative forms for efficient computation of the iterative EI method are presented. Finally, both methods are applied to the I-40 Bridge located over the Rio Grande in Albuquerque, New Mexico, and the derived relationship is verified.

1. Introduction

Before outlining the paper, we describe the motivations, introduce the basics of the two sensor placement methods, and discuss their differences and connections.

1.1. Motivations

The problem of sensor placement is an importance issue in dynamic testing of large structures, and has been investigated from different approaches, as can be seen from the abundance of literature [1–3], and the references therein. Especially due to the increasing interest of damage identification and structural health monitoring (SHM) in last two decades, more researchers are involved in this topic, and methods from various perspectives are proposed [4,5]. The key ideas behind these approaches are, however, similar. Most sensor placement methods aim to achieve best sensitivity changes' detection of signatures indicating damage, or the

*Corresponding author. Dalian University of Technology, State Key Laboratory of Coastal and Offshore Engineering, School of Civil and Hydraulic Engineering, Ganjingzi district, Linggong Road 2, Dalian 116023, China. Tel: +86 (411) 84708512x8217; fax: +86 (411) 84708501.
E-mail address: dsli@dlut.edu.cn (D.S. Li).

0022-460X/$ - see front matter
doi:10.1016/j.jsv.2007.05.004

best identification of structural characteristics, including the eigenfrequencies, mode shapes, and also damping ratios. Although a single eigenfrequency or mode shape is not definitely sensitive and sufficient enough for detecting the existence of damage in SHM, the combination of them, such as those used in subspace-based damage identification method [6], shows great potentials. In this connection, the eigenfrequencies and the mode shapes are to be identified as accurately as possible, and server as a benchmark database for the following model updating, and damage identification. This is the objective of the two methods to be discussed, the modal kinetic energy (MKE) and the effective independence (EI) method, which is the most influential and commonly used. The EI is recommend by Ewins [7], Heylen et al. [8], and Friswell and Mottershead [9] for modal testing and modal updating, and already embedded in commercial software MSC/NASTRAN [10].

Although the theory of both MKE and EI methods are quite straightforward and well developed, and both are widely discussed and applied, the same degree of understanding cannot be said to exist. Researchers may notice that EI can arrive at similar results as that of MKE in many circumstances, and may have a vague feeling that MKE and EI have something in common. Their relationship, which was thought to be important on the basis of theoretical considerations and on the development of other effective sensor placement methods, is not explicitly and mathematically reported. This is the topic of our present work. From the viewpoint of the authors, the difference and consistency of MKE and EI will increase the understanding of both methods, and the role of each candidate sensor position played in EI.

1.2. Problem formulation of sensor placement

The sensor placement problem can be investigated from uncoupled modal coordinates of governing structural equations as follows:

$$\begin{aligned}&\ddot{\mathbf{q}}_i + \mathbf{M}_i^{-1}\mathbf{C}_i\dot{\mathbf{q}}_i + \mathbf{M}_i^{-1}\mathbf{K}_i\mathbf{q}_i = \mathbf{M}_i^{-1}\mathbf{\Phi}^{\mathrm{T}}\mathbf{B}_0\mathbf{u},\\ &\mathbf{y} = \mathbf{\Phi}\mathbf{q} + \boldsymbol{\varepsilon},\end{aligned} \tag{1}$$

where $\mathbf{q}_i$ is the ith modal coordinate and is also the ith element of the vector, $\mathbf{q}$, in the 2nd equation, $\mathbf{M}_i$, $\mathbf{K}_i$ and $\mathbf{C}_i$ are the corresponding ith modal mass, stiffness and damping matrix, respectively, $\mathbf{\Phi}$ is the mode shape matrix with its ith column as the ith mass-normalized mode shape, $\mathbf{B}_0$ is simply a location matrix formed by ones (corresponding to actuators) and zeros (no loadings), specifying the positions of the force vector $\mathbf{u}$. The superscripts $^{-1}$ and $^{\mathrm{T}}$ represent inversion and transpose of a matrix, respectively. $\mathbf{y}$ is a measurement column vector indicating which positions of the structure are measured, and $\boldsymbol{\varepsilon}$ is a stationary Gaussian white noise with zero mean and a variance of $\mathbf{\Psi}_0^2$.

Sensor placement problem described in Model (1) is, essentially, divided into three aspects. Firstly, what is the least number of accelerometers required to be installed in a structure for a successful dynamic testing? Secondly, where should these accelerometers be installed, including those additional ones if available? And if these additional sensors are available, should we install them as redundant sensors or place them in other positions? Lastly, how could we evaluate the effectiveness of different sensor placement methods?

The first problem is partly resolved. It is known that the minimum number of sensors to be instrumented could not be less than the number of mode shapes to be identified, which is determined by the observability of the system. Moreover, the practical number of sensors, which is limitedly preset before test due to the availability of instruments, is usually larger than the minimum number because of the requirement to visualize the identified mode shapes [11].

The second problem is the core and amazing one, which depends largely, however, on the third aspect. As mentioned in the introduction, the MKE and EI methods discussed in this paper aim both to the best identification of the eigenfrequencies and mode shapes. There are, of course, other objectives for sensor placement, for instance, to decrease the uncertainties of parameters to be identified [12–13], to increase mutual information [14]. A specific objective depends on its applications. We will not discuss further the third aspect of the sensor placement problem in this paper, which is beyond the current scope. Therefore, only the second problem is left, and is the focus of this work. Without loss of generality, it is assumed here that the total degrees of freedom (dofs) of the structure described in Model (1) is n, the number of mode shapes used for sensor placement is k, and the available number of sensors is m. Then the sensor placement problem becomes, basically, where to deploy the m available sensors out of the total n dofs of a structure for dynamic testing, i.e. which rows of the measurement vector $\mathbf{y}$ in Eq. (1) are to be selected. MKE and EI give apparent different solutions to this problem. However, there is an underlying connection between these two solutions, which is unknown before and will be discussed in this paper.

1.3. Outline of the paper

This paper is structured as follows. Section 2 describes the rationale and basis of the MKE and EI methods. In Section 3, the connection of both methods is derived, and the physical significance of the EI method is recapitulated. Section 4 discusses the effect of non homo-generous mass distribution on MKE, and the computation aspects of EI. In Section 5, both MKE and EI are applied on the I-40 Bridge to verify their connection. Finally, the results and contributions of this paper are presented.

2. MKE and EI

Both MKE and EI methods have found many applications in actual dynamic testing, and obtained reasonable results. Their theoretical background and rationale are to be explained in this section. The material presented here is well known [1–3], and expounded repeatedly for the sake of clarity and our derivation of their relationship in Section 3.

2.1. The MKE method

The MKE provides a rough measure of the dynamic contribution of each candidate sensor to the target mode shapes. The reason to adopt MKE resides in that it tells which dofs capture most of the relevant dynamic features of the structure. MKE helps to select those sensor positions with possible large amplitudes, and to increase the signal to noise ratio, which is critical in harsh and noisy circumstances [2,3].

The method ranks all candidate sensor positions by their MKE indices as follows:

$$\mathrm{MKE}_{pq} = \mathbf{\Phi}_{pq} \sum_{s=1}^{n} \mathbf{M}_{ps} \mathbf{\Phi}_{sq} \tag{2}$$

where MKE_{pq} is the kinetic energy associated with the pth dof in the qth target mode, $\mathbf{\Phi}_{pq}$ is the pth component in the corresponding qth mode shape, $\mathbf{M}_{pq}$ is the term in the pth row and sth column of the mass matrix $\mathbf{M}$, and $\mathbf{\Phi}_{sq}$ is the sth coefficient in the qth target mode shape. The sensor locations with higher values of MKE are selected as measurement sensor set.

2.2. The EI method

The aim of the EI method is to select measurement positions that make the mode shapes of interest as linearly independent as possible while containing sufficient information about the target modal responses in the measurements [2,15–18]. The method originates from estimation theory by sensitivity analysis of the parameters to be estimated, and then it arrives at the maximization of the Fisher information matrix, for instance, the determinant or the trace, as well as to minimize the condition number of the information matrix. It is reflected in the coefficient variance–covariance matrix. Thus, the covariance matrix of the estimate error of the modal coordinates would be minimized. The number of sensors is reduced from an initially large candidate set in an iterative manner by removing sensors from those dofs, which contribute least among all the candidate sensors to the linear independence of the target modes. In the end, it preserves the required necessary candidate sensors as the optimal sensor set.

From the measurement output expression in Eq. (1), the EI analyzes the covariance matrix of the estimate error for an efficient unbiased estimator as follows:

$$E\left[(\mathbf{q}-\hat{\mathbf{q}})(\mathbf{q}-\hat{\mathbf{q}})^{\mathrm{T}}\right]=\left[\left(\frac{\partial \mathbf{y}}{\partial \mathbf{q}}\right)^{\mathrm{T}}\left[\mathbf{\Psi}_0^2\right]^{-1}\left(\frac{\partial \mathbf{y}}{\partial \mathbf{q}}\right)\right]^{-1}=\left[\frac{1}{\mathbf{\Psi}_0^2}\mathbf{\Phi}^{\mathrm{T}}\mathbf{\Phi}\right]^{-1}=\mathbf{Q}^{-1}, \tag{3}$$

in which $\mathbf{Q}$ is the Fisher information matrix, $\mathbf{\Psi}_0^2$ represents the variance of the stationary Gaussian measurement white noise $\boldsymbol{\varepsilon}$ in Eq. (1), E denotes the expected value, and $\hat{\mathbf{q}}$ is the efficient unbiased estimator of $\mathbf{q}$. Maximizing $\mathbf{Q}$ will result in the best state estimate of $\mathbf{q}$. In practice, the analysis begins by solving the following eigenvalue equation:

$$\left[\mathbf{\Phi}^{\mathrm{T}}\mathbf{\Phi}-\lambda \mathrm{I}\right]\boldsymbol{\psi}=0, \tag{4}$$

where $\boldsymbol{\psi}$ are the orthogonal eigenvectors. The EI coefficients of the candidate sensors are computed by the following formation:

$$E_D=[\mathbf{\Phi}\boldsymbol{\psi}]\otimes[\mathbf{\Phi}\boldsymbol{\psi}]\lambda^{-1}\cdot\mathbf{1}, \tag{5}$$

in which $\otimes$ represents a term-by-term matrix multiplication, $\mathbf{1}$ is an $n\times 1$ column vector with all elements of 1. E_D is the EI indices, which evaluate the contribution of a candidate sensor location to the linear independence of the modal partitions $\mathbf{\Phi}$.

The selection procedure is to sort the elements of the E_D coefficients, and to remove the smallest one at a time. The E_D coefficients are then updated according to the new modal shape matrix, and the process is repeated iteratively until the number of remained sensors equals to a preset value. The remained dofs serve as the measurement locations, referring to Kammer [2] for details of the EI theory.

3. The relationship between MKE and EI methods

In previous investigations of comparisons among different sensor placement methods [2,3,15–18], the EI and MKE show similar results, especially for the first several iterations of the EI and MKE in the cases of structures with homogeneous mass distributions. However, the connection between both influential methods is not clearly understood, at least to the knowledge of the authors from the literature. In this section, the latent connection between both methods is revealed.

For simplicity to expose the relationship between MKE and EI, an identity equivalent mass matrix is assumed at first, and then the effects of non-identity equivalent mass matrix on sensor placement will be discussed in Section 4. Under the assumption of an identity equivalent mass matrix and normalized mode shapes with respect to the mass matrix, the MKE index can be rewritten as the following formula:

$$\mathrm{MKE}=\mathrm{diag}(\mathbf{\Phi}\mathbf{\Phi}^{\mathrm{T}}), \tag{6}$$

where operator diag denotes a column vector formed by the diagonal terms of a matrix. Similarly, the EI index can be alternatively computed as the diagonal of the following matrix [2]:

$$E_D=\mathrm{diag}(\mathbf{\Phi}\left[\mathbf{\Phi}^{\mathrm{T}}\mathbf{\Phi}\right]^{-1}\mathbf{\Phi}^{\mathrm{T}}). \tag{7}$$

From the above Eqs. (6) and (7), it can be certainly observed that the result of the first iteration of EI should be the same as that of the MKE, which is already shown clearly in the examples of references using EI methods [2,3,15–18]. This is simply due to the fact that the mode shape matrix is normalized in the first iteration of EI, and the middle term in the right-hand side of Eq. (7) is just an identity matrix. The two formations of EI and MKE are identical under this circumstance. It is, therefore, unnecessary to apply MKE first when implementing EI as originally proposed by Kramer [2]. In the following iterations, the EI indices are weighted by an inversion term of the reduced Fisher information matrix, but the MKE is not. And this is why EI is different from MKE afterwards.

When the EI in the second iteration is considered, we found that the measured sensor output formulated in Eq. (1) should be rewritten because a previously assumed output component is not measured anymore. Without loss of generality, the kth index of EI in Eq. (7) in the first iteration is assumed to be the smallest and to be excluded. Then, the reduced output vector in Eq. (1) should be reformulated as follows:

$$\mathbf{y}_1 = \mathbf{\Phi}_1\mathbf{q}_1 + \mathbf{\varepsilon}_1, \tag{8}$$

where, $\mathbf{y}_1$ denotes the remained measurements with the kth measurement deleted in $\mathbf{y}$ of the Eq. (1), and $\mathbf{\varepsilon}_1$ is the corresponding stationary Gaussian measurement white noise, and likewise, $\mathbf{\Phi}_1$is the same mode shape matrix as $\mathbf{\Phi}$ in Eq. (1) only with the kth row deleted, $\mathbf{q}_1$ is a new modal coordinate vector with the same dimensions as that of $\mathbf{q}$ in Eq. (1). The model described in Eq. (8) becomes a reduced system with only $n-1$ dofs since the previous kth dof in the original model is rejected.

Basically, we view sensor placement broadly as a problem of system reduction, and the low-dimensional reduced system defined in Eq. (8) is to represent the original full-scale system in Eq. (1) as exactly as possible. The information discarded by excluding $n-k$ sensor positions should be insignificant compared to the k sensors retained.

In this new reduced system with order of $n-1$, the mode shape matrix should be renormalized as the original system. Following the same procedures similar from Eq. (3) to Eq. (5) with ortho-normalized mode shapes ($\mathbf{\Phi}_1^{\mathrm{T}}\mathbf{\Phi}_1 = \mathbf{I}$), a formulation with the same rationale can be easily obtained:

$$E_{D1} = \mathrm{diag}(\mathbf{\Phi}_1\left[\mathbf{\Phi}_1^{\mathrm{T}}\mathbf{\Phi}_1\right]^{-1}\mathbf{\Phi}_1^{\mathrm{T}}) = \mathrm{diag}(\mathbf{\Phi}_1\mathbf{\Phi}_1^{\mathrm{T}}). \tag{9}$$

The EI index in Eq. (9) is degenerated once again in form into the MKE index of Eq. (6) in its 2nd iteration. Therefore, the key difference between EI and MKE is that in the following iterations of EI, the reduced mode shape matrix is not renormalized, but the MKE is initially using an already normalized mode shape matrix. A reorthonormalized EI in its iterations is merely MKE.

To strengthen our arguments further, we consider a special case, in which only one mode shape is considered to compute for sensor placement by MKE and EI, respectively. In this case, the MKE indices are simply the squares of the mode shape components corresponding to the sensor positions in Eq. (6), i.e. $\mathrm{MKE}_i = \mathbf{\Phi}_i^2$, and the EI indices ($E_{Di} = \mathbf{\Phi}_i^2/(\sum_{i=1}^{n}\mathbf{\Phi}_i^2)$) are the squares of the mode shape components only divided by a constant (the squared Euclidean norm of the mode shape according to Eq. (7)). The only difference between both indices is a constant coefficient. Their ranked sequence is the same, no matter how many sensors are to be used.

We can now consider EI from another viewpoint. The mode shapes used in EI, regardless of ortho-normalized or not, can be decomposed using orthogonal–triangular decomposition (**QR**) as follows [19–21]:

$$\mathbf{\Phi} = \mathbf{QR}, \tag{10}$$

where $\mathbf{Q}$ is an $n \times k$ unitary matrix with the same dimensions as $\mathbf{\Phi}$, and $\mathbf{R}$ is a $k \times k$ upper triangular matrix. Thus, the EI index can be also computed using the above decomposed $\mathbf{Q}$ and $\mathbf{R}$ matrix by substituting Eq. (10) into Eq. (7):

$$E_D = \mathrm{diag}(\mathbf{QR}\left[\mathbf{R}^{\mathrm{T}}\mathbf{Q}^{\mathrm{T}}\mathbf{QR}\right]^{-1}\mathbf{R}^{\mathrm{T}}\mathbf{Q}^{\mathrm{T}}) = \mathrm{diag}(\mathbf{QQ}^{\mathrm{T}}). \tag{11}$$

The expression of EI in Eq. (11) is the same in form as that of MKE in Eq. (6). In each iteration of EI, it computes "MKE index" using the reduced ortho-normalized mode shapes, retains dofs with large MKEs, and deletes those with small MKEs.

The rationale behind the **QR** decomposition in Eq. (10) is the same as the above reasoning for the idea of viewing sensor placement as system reduction. **QR** decomposition is, in fact, an extension of the Gram–Schmidt orthogonalization applying to the dependent columns of reduced mode shapes $\mathbf{\Phi}_1$, which is not strictly orthogonal anymore after certain row of the previous orthogonal mode shapes is deleted in the proceeding iteration. Consequently, the **QR** decomposition in Eq. (10) extracts an orthogonal subspace spanned by the columns of $\mathbf{Q}$. The $\mathbf{Q}$ in Eq. (10) is an $n \times k$ ortho-normal matrix. This means that the columns of the reduced mode shape matrix $\mathbf{\Phi}_1$ resulted from iterations of EI will be remapped onto the subspace spanned by the ortho-normalized columns of $\mathbf{Q}$. And it is exactly these columns of $\mathbf{Q}$ that will combine to form the reduced measurement vector $\mathbf{y}$. In dynamic testing, it is also these columns of $\mathbf{Q}$ that are identified as mode shapes of the reduced system being measured.

As a result, the difference and consistency between MKE and EI is clear. EI requires iteration computations, but MKE does not. In the following iterations of EI, it redistributes the MKE into the retaining dofs and recomputed their MKE index for the reduced system using re-orthonormalized mode shapes. EI is an iterated version of MKE with re-orthonormalized mode shapes.

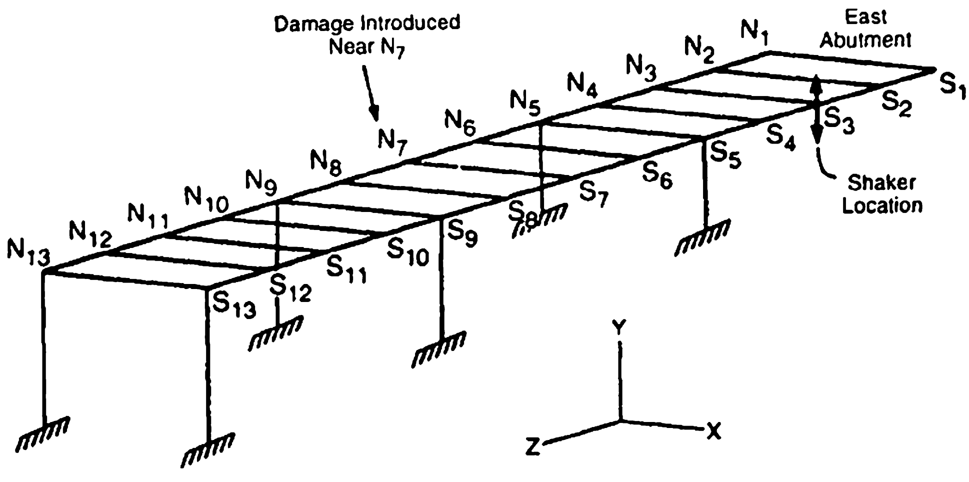

Fig. 1. Location of shaker and accelerometers of the I-40 Bridge.

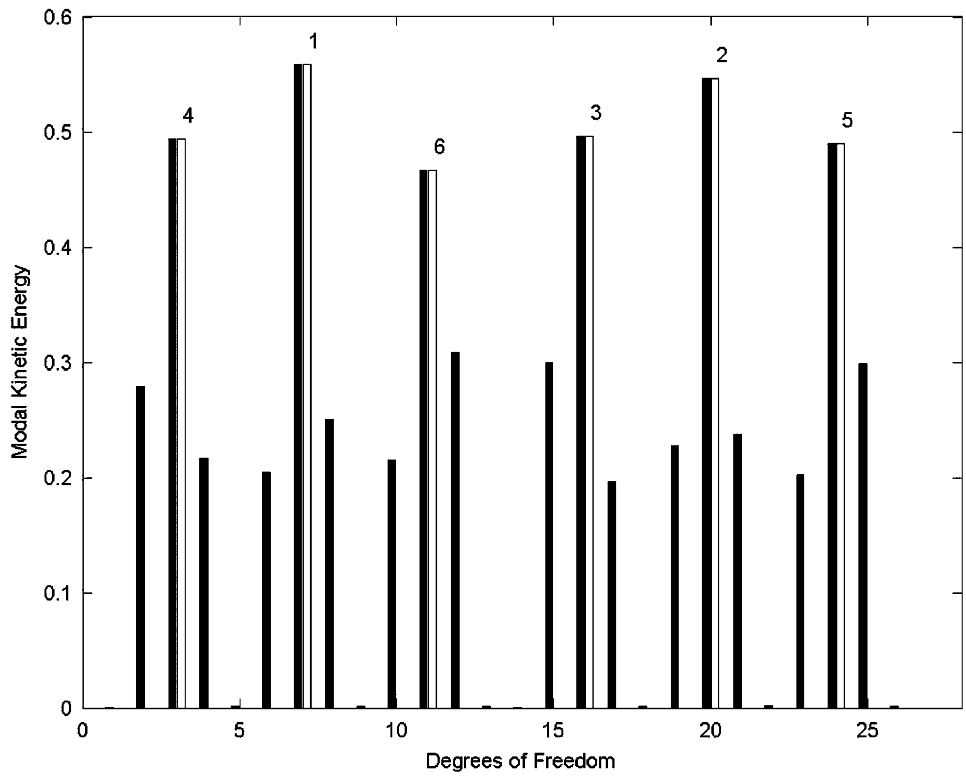

Fig. 2. Modal kinetic energy distribution. Black column: MKE indices for all candidate sensor positions; white column: MKE indices of selected 6 dofs, right upper numbers indicate the sequence of their relative importance.

4. Mass distribution effects

For cases of non-identity equivalent mass matrix, the above reasoning can be generalized. The MKE index is computed by

$$\mathrm{MKE} = \mathrm{diag}(\mathbf{M}\mathbf{\Phi}\mathbf{\Phi}^{\mathrm{T}}) = \mathrm{diag}(\mathbf{M}^{1/2}\mathbf{\Phi}\mathbf{\Phi}^{\mathrm{T}}\mathbf{M}^{1/2}), \tag{12}$$

where $\mathbf{M}^{1/2}$ is the square root of the semi-definite mass matrix $\mathbf{M}$. In MKE, each candidate dof is weighted by the corresponding component in the mass matrix. For those dofs associated with large components in the mass matrix, they are given more weights in the ranking of their importance for sensor placement. Hence, MKE reflects the characteristics of mass distribution for a given structure.

Moreover, the EI index can still be computed using Eq. (7) regardless of mass distribution. To analyze the iterations of EI, the Sherman–Morrision-formula can be employed [19]:

$$\left[\mathbf{\Phi}_{(i)}^{\mathrm{T}}\mathbf{\Phi}_{(i)}\right]^{-1} = \left[\mathbf{\Phi}^{\mathrm{T}}\mathbf{\Phi} - \mathbf{\Phi}_i\mathbf{\Phi}_i^{\mathrm{T}}\right]^{-1} = \left[\mathbf{\Phi}^{\mathrm{T}}\mathbf{\Phi}\right]^{-1} + \frac{\left[\mathbf{\Phi}^{\mathrm{T}}\mathbf{\Phi}\right]^{-1}\mathbf{\Phi}_i\mathbf{\Phi}_i^{\mathrm{T}}\left[\mathbf{\Phi}^{\mathrm{T}}\mathbf{\Phi}\right]^{-1}}{1 - \mathbf{\Phi}_i^{\mathrm{T}}\left[\mathbf{\Phi}^{\mathrm{T}}\mathbf{\Phi}\right]^{-1}\mathbf{\Phi}_i}, \tag{13}$$

where $\mathbf{\Phi}_{(i)}$ is the same mode shape matrix as $\mathbf{\Phi}$ only with the ith row deleted, $\mathbf{\Phi}_i$ is a column vector that is the transpose of the ith row of the mode shape matrix $\mathbf{\Phi}$ to be deleted in an iteration of EI. The EI index can be computed using Eq. (13) to facilitate the inversion of the middle term in Eq. (7) in the following iterations.

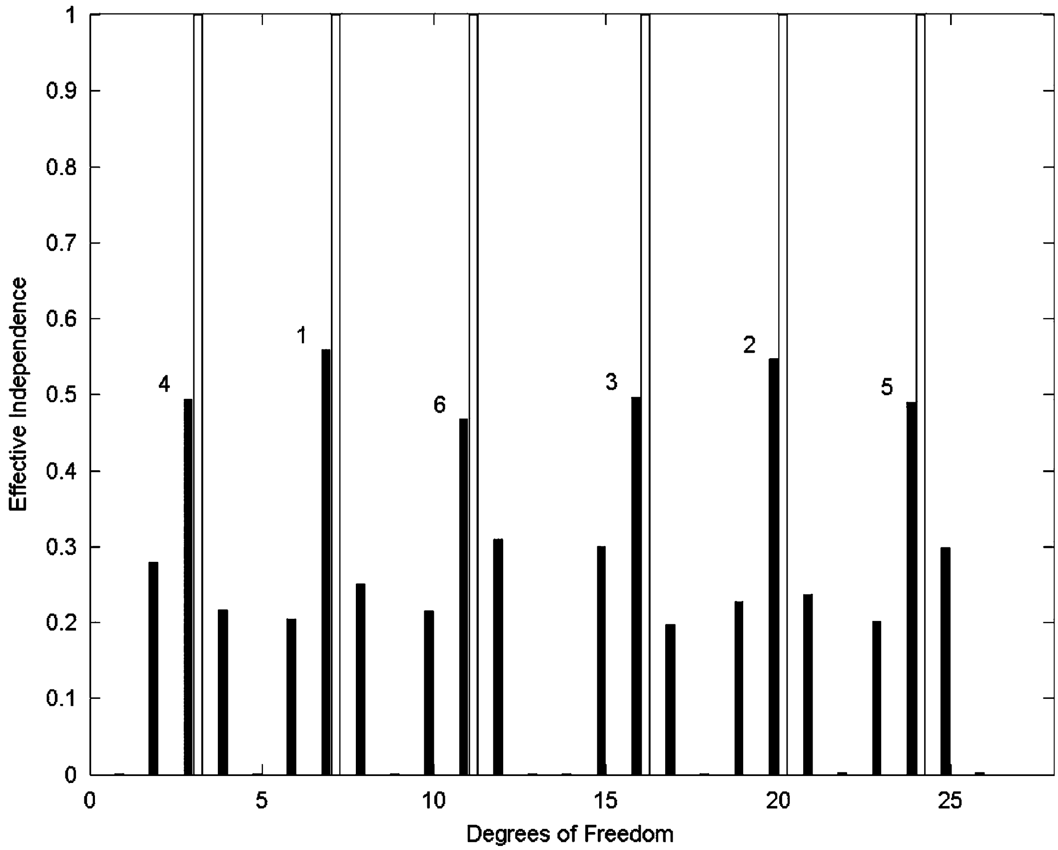

Fig. 3. Effective independence distribution. Black column: first EI iteration, left upper numbers indicate the sequence of their relative importance; white column: final EI indices of selected 6 dofs.

Since the mode shapes in the original system is ortho-normalized, Eq. (13) in the first iteration of EI is reduced to

$$\left[\mathbf{\Phi}_{(i)}^{\mathrm{T}}\mathbf{\Phi}_{(i)}\right]^{-1} = \mathbf{I} + \frac{\mathbf{\Phi}_i\mathbf{\Phi}_i^{\mathrm{T}}}{1-\mathbf{\Phi}_i^{\mathrm{T}}\mathbf{\Phi}_i}. \tag{14}$$

It is obvious that the left-hand side of Eq. (14) does not deviate much from an identity matrix because the EI method selects a row with a smallest norm in the original mode shape matrix to delete. The second term in the right-hand side of Eq. (14) is just a small perturbation matrix and insignificant. At least the inverse in Eq. (14) is a diagonal dominant matrix. Hence, the inverse middle term in Eq. (7) can be regarded as weights for the mode shapes of a reduced system after certain dofs have been sequentially deleted. Therefore, the EI method adds different weights for the remaining mode shapes during its iterations, whereas MKE adds weights for each candidate dof.

Pre-multiplying both sides of Eq. (13) with $\mathbf{\Phi}_r$ and post-multiplying with $\mathbf{\Phi}_r^{\mathrm{T}}$, we can obtain a simple efficient expression for the iterative computation of the EI index:

$$h_{rr(i)} = h_{rr} + \frac{h_{ri}^2}{1-h_{ii}}, \tag{15}$$

where $h_{rr(i)}$ is the rth diagonal term of the expression in the bracket of the right hand side of Eq. (7) with the ith row of the mode shape matrix in $\mathbf{\Phi}$ deleted, and h_{rr} is the rth diagonal term of the full mode shape matrix $\mathbf{\Phi}$, and likewise h_{ii} and h_{ri}. The h_{rr} is called as leverage of each predicted value on its actual measurement $\mathbf{y}$ in statistics [20]. As stated above, the EI method iterates to delete rows corresponding to small h_{ii}. The iterative

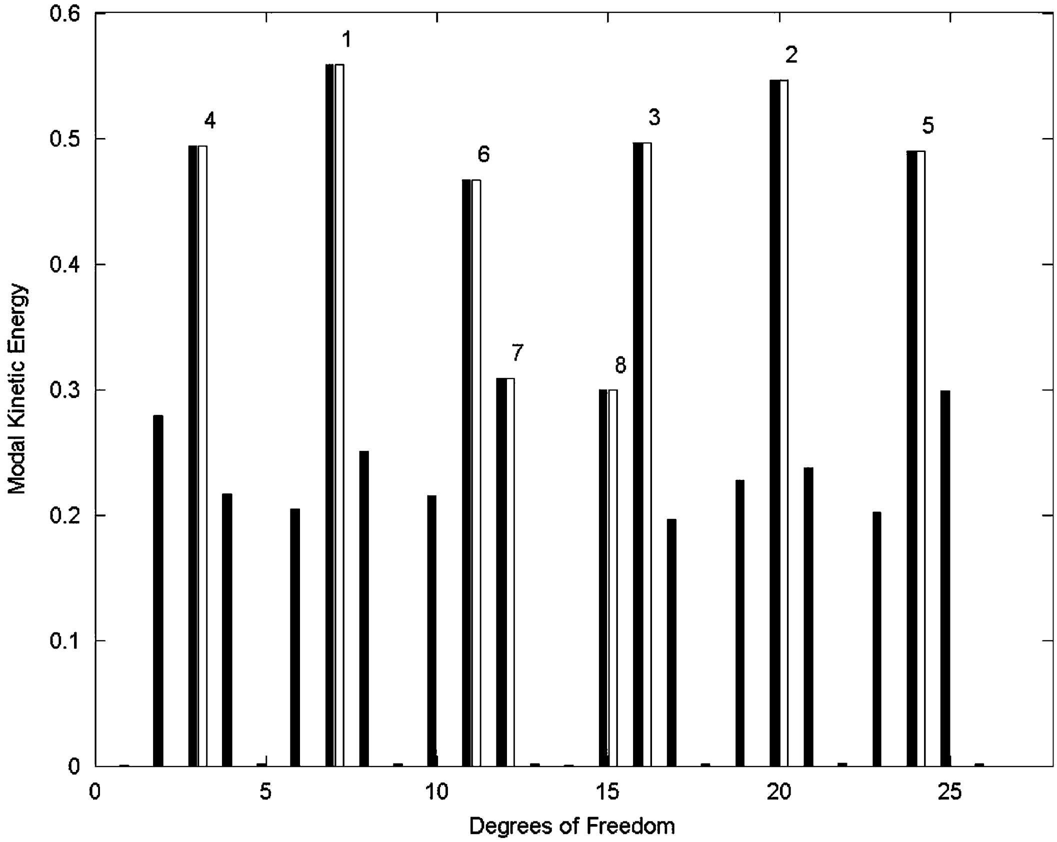

Fig. 4. Modal kinetic energy distribution. Black column: MKE indices for all candidate sensor positions; white column: MKE indices of selected 8 dofs, right upper numbers indicate the sequence of their relative importance.

EI index, the change of the EI index after the ith row of the previous mode shape matrix is deleted, can be efficiently computed using Eq. (15) without the computational burden of matrix inversion.

5. Application to the I-40 Bridge

The application of both MKE and EI is demonstrated using the measurement data of the I-40 Bridge, located over the Rio Grande in Albuquerque, New Mexico. The I-40 Bridge consists of twin spans made up of a concrete deck supported by two welded-steel plate girders and three steel stringers. The tested section has three spans. The end spans are of equal length, approximately 39.9 m, and the center span is approximately 49.4 m long.

There are in total 13 accelerometers used along the length of the bridge, for a total of 26 responses. The shaker consists of a 96.5 kN reaction mass supported by three air springs resting on top of drums filled with sand. The shaker was located on the eastern-most span directly above the south plate girder and midway between the abutment and first pier. Fig. 1 shows the shaker and accelerometer locations. Full details of the modal testing of this bridge can be found in Farrar et al. [22].

The mode shapes extracted from the case of "Test t11tr" are used for the computation of sensor placement of both MKE and EI. In this bridge, there are in total 26 dofs ($n = 26$), and 6 identified mode shapes ($k = 6$) available. Three cases are considered in this paper. In Case 1, 25 accelerometers will be deployed ($m = 25$). This case corresponds to the first iteration of EI. In Case 2, 6 accelerometers will be used ($m = 6$). The number of accelerometers used in Case 2 is the minimum number to identify the 6 mode shapes. In Case 3, 8 accelerometers will be used ($m = 8$).

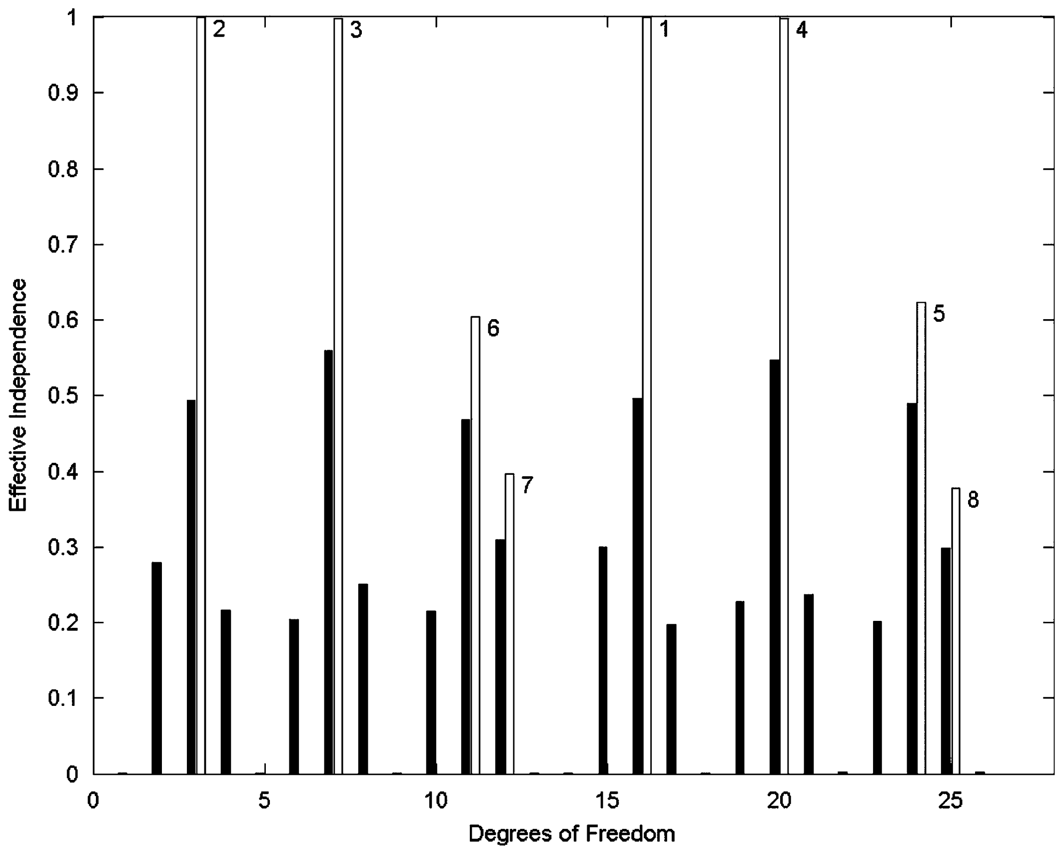

Fig. 5. Effective independence distribution. Black column: first EI iteration; white column: final EI indices of selected 8 dofs, right lower numbers indicate the sequence of their relative importance.

In Case 1, both MKE and EI pick sensor position "S1" for exclusion, and their ranking sequences are identical. For Case 2, the ranking sequence of MKE (Fig. 2) in descending order is S7, N7, N3, S3, N11, and S11. The dofs in horizontal axis of Fig. 2, as well as Figs. 3–5, are numbered as 1, 2, …, 13 for candidate sensor positions S1, S2, …, S13 in Fig. 1, and 14, 15, …, 26 for N1, N2, …, N13, respectively. As shown in Fig. 3, the same six sensor positions chosen by MKE are also selected by EI. However, their relative importance is different from that of MKE. In EI, the six sensor positions are of equal importance since their EI indices are all 1 as shown by the white columns in Fig. 3. It is worth to note that all the middle-span positions are picked up by both MKE and EI in Case 2. Moreover, the numbers on the left upper corner of the black columns in Fig. 3 indicate the EI indices in its first iteration. The six sensor positions are ranked in the same order of importance by EI (Fig. 3) as by MKE (Fig. 2), note the different vertical scales. The first iterations of both MKE and EI result in the same candidate sensor sequence for both Cases 1 and 2. This agrees with our derivation in Section 4, the outcome of the first iteration of EI should be the same as that of the MKE.

Figs. 4 and 5 show the results of MKE and EI in Case 3. By MKE, the selected 8 sensor positions are S7, N7, N3, S3, N11, S11, S12, and N2, whereas the selected 8 sensor positions by EI are N3, S3, S7, N7, N11, S11, S12, and N12. Both sequences are given in descending order of relative importance, as determined by their MKE or EI indices. The essential difference between MKE and EI resides in the 8th sensor. It turns out MKE selects N2 as its 8th sensor, whereas EI chooses N12. It shows clearly that not only the selected sensors are different by MKE and EI, but their relative importance are not in the same order, even for the first 5 sensors that are identified both by MKE and EI. This verifies further the observation in the end of Section 5 that EI iteratively redistributes the MKE into the retaining dofs, and reranks their relative importance.

6. Conclusions

Two influential sensor placement methods, i.e. modal kinetic energy (MKE) method and effective independence (EI) method, are discussed and compared, and the connection between the two methods is derived. MKE ranks the relative importance of all candidate dofs by their kinetic energy with the mass distribution associated with each dof as weights. EI is an iterated version of MKE with re-orthonormalized mode shapes regardless of mass distribution of a structure. It is found that the latter is an iterated version of the former for the case of a structure with equivalent identity mass matrix.

The application of MKE and EI on the I-40 Bridge demonstrate their connections. Although both MKE and EI give similar results for the cases of sensor number 25, and 6, they select different sensor combinations for the case of sensor number 8.

Furthermore, this paper provides two efficient alternative forms to compute the EI index. One is the stable QR method as shown in Eq. (11), and the other is the iterative row deletion method in Eq. (15).

Acknowledgments

The authors are indebted to the editor, Professor Christopher Morfey, and the referees, whose careful reading and comments helped improving an earlier version of the paper. The authors are grateful for the joint support of China Natural Science Foundation (No. 50408031), and German Academic Exchange Service (DAAD).

References

[1] F.E. Udwadia, Methodology for optimum sensor locations for parameter identification in dynamic systems, *Journal of Engineering Mechanics* 120 (2) (1994) 368–390.

[2] D.C. Kammer, Sensor placement for on-orbit modal identification and correlation of large space structures, *Journal of Guidance, Control and Dynamics* 14 (1991) 251–259.

[3] M. Papadopoulos, E. Garcia, Sensor placement methodologies for dynamic testing, *AIAA Journal* 36 (2) (1998) 256–263.

[4] D. Balageas, C.P. Fritzen, A. Güemes, *Structural Health Monitoring*, ISTE, London, UK, 2006.

[5] D.S. Li, H.N. Li, C.P. Fritzen, On the physical significance of the norm based sensor placement method, *Proceedings of the Third European Workshop on Structural Health Monitoring*, Granada, Spain, 5–7 July 2006, pp. 1542–1550.

[6] M. Basseville, M. Abdelghani, A. Benveniste, Subspace-based fault detection algorithms for vibration monitoring, *Automatica* 36 (1) (2000) 101–109.
[7] D.J. Ewins, *Modal Testing; Theory, Practice, and Application*, Research Studies Press, London, UK, 2000.
[8] W. Heylen, S. Lammens, P. Sas, *Modal Analysis Theory and Testing*, Katholeike University Leuven, Belgium, 1998.
[9] M.I. Friswell, J.E. Mottershead, *Finite Element Model Updating in Structural Dynamics*, Dordrecht, Kluwer, 1995.
[10] J. Peck, I. Torres, A DMAP Program for the selection of accelerometer locations in MSC/ NASTRAN, *Proceedings of the 45th AIAA/ASME/ASCE/AHS/ASC Structures, Structural Dynamics and Materials Conference*, Palm Springs, CA, United States, 2004, pp. 19–22.
[11] C.R. Pickrel, A practical approach to modal pretest design, *Mechanical Systems and Signal processing* 13 (2) (1999) 271–295.
[12] C. Papadimitriou, Optimal sensor placement methodology for parametric identification of structural systems, *Journal of Sound and Vibration* 278 (4) (2004) 923–947.
[13] E. Heredia-Zavoni, L. Esteva, Optimal instrumentation of uncertain structural systems subject to earthquake ground motions, *Earthquake Engineering and Structural Dynamics* 27 (4) (1998) 343–362.
[14] I. Trendafilova, W. Heylen, H. Van Brussel, Measurement point selection in damage detection using the mutual information concept, *Smart Materials and Structures* 10 (3) (2001) 528–533.
[15] D.C. Kammer, M.L. Tinker, Optimal placement of tri-axial accelerometers for modal vibration tests, *Mechanical systems and signal processing* 18 (2004) 29–41.
[16] G. Heo, M.L. wang, D. Satpathi, Optimal transducer placement for health monitoring of long span bridge, *Soil Dynamics and Earthquake Engineering* 16 (1997) 495–502.
[17] M. Meo, G. Zumpano, On the optimal sensor placement techniques for a bridge structure, *Engineering Structures* 27 (2005) 1488–1497.
[18] Glassburn, R.S., 1994. Evaluation of sensor placement algorithms for on-orbit identification of space platforms, Master Thesis, Department of mechanical engineering, University of Kentucky, USA.
[19] P.E. Gill, W. Murray, M.H. Wright, *Numerical Linear Algebra and Optimization*, Addison-Wesley, Redwood City, CA, USA, 1991.
[20] R.D. Cook, S. Weisberg, *Residuals and Influence in Regression*, Chapman & Hall, London, 1982.
[21] R.A. Horn, C.R. Johnson, *Matrix Analysis*, Cambridge University Press, London, 1990.
[22] C. R. Farrar, W.E. Baker, T.M. Bell, K.M. Cone, T.W. Darling, T.A. Duffey, A. Eklund, A. Migliori, Dynamic characterization and damage detection in the I-40 Bridge over the Rio Grande, Los Alamos National Laboratory Report LA-12767-MS, June 1994.